

# Determinants of the *Drosophila* Odorant Receptor Pattern

Erin Song,<sup>1</sup> Benjamin de Bivort,<sup>1,2</sup> Chuntao Dan,<sup>1,3</sup> and Sam Kunes<sup>1,\*</sup>

<sup>1</sup>Department of Molecular and Cellular Biology, Harvard University, Cambridge, MA 02138, USA

<sup>2</sup>Present address: Rowland Institute at Harvard, 100 Edwin Land Boulevard, Cambridge, MA 02142, USA

<sup>3</sup>Present address: Janelia Farm Research Campus, 19700 Helix Drive, Ashburn, VA 20147, USA

\*Correspondence: [kunes@fas.harvard.edu](mailto:kunes@fas.harvard.edu)

DOI 10.1016/j.devcel.2011.12.015

## SUMMARY

In most olfactory systems studied to date, neurons that express the same *odorant receptor (Or)* gene are scattered across sensory epithelia, intermingled with neurons that express different *Or* genes. In *Drosophila*, olfactory sensilla that express the same *Or* gene are dispersed on the antenna and the maxillary palp. Here we show that *Or* identity is specified in a spatially stereotyped pattern by the cell-autonomous activity of the transcriptional regulators Engrailed and Dachshund. Olfactory sensilla then become highly motile and disperse beneath the epidermis. Thus, positional information and cell motility underlie the dispersed patterns of *Drosophila* *Or* gene expression.

## INTRODUCTION

Despite the catalog of mechanisms known to determine cell fate, how an olfactory receptor neuron (ORN) chooses to express a particular *odorant receptor (Or)* gene remains unclear. In most olfactory systems studied to date, neurons that express the same *Or* family member are scattered across sensory epithelia, interspersed with neurons that express different *Or* genes (Ressler et al., 1993; Vassar et al., 1993; Vosshall et al., 1999; Ngai et al., 1993). These patterns are similar but not identical between individuals and might be explained by stochastic mechanisms whereby distant neurons independently select an *Or* gene from a regionally restricted palette (reviewed in Fuss and Ray, 2009). There is evidence for such a mechanism in the mouse, where a distal enhancer element (the H domain) activates one of at least several possible *Or* loci (Serizawa et al., 2003; Lomvardas et al., 2006; Fuss et al., 2007). It is not clear, however, if stochastic mechanisms are universal determinants of *Or* gene choice.

Olfactory epithelia in *Drosophila* are found on the third segment of the antenna and the maxillary palp. Together these tissues contain 2,000–3,000 odorant receptor neurons (ORNs), which are organized into ~1,100 sensillum units (Shanbhag et al., 2000). *Drosophila* sensilla come in a number of defined types, each with characteristic odorant response spectra (Clyne et al., 1997; de Bruyne et al., 1999, 2001) due to stereotyped patterns of *Or* gene expression (Hallem et al., 2004; Goldman

et al., 2005; Couto et al., 2005; Fishilevich and Vosshall, 2005). Most ORNs express one *Or* chosen from a library of 60 *Or* genes, whereas others express a member of the ionotropic glutamate receptor-like family (Benton et al., 2009). All *Or* genes are expressed in conjunction with *Or83b* (Larsson et al., 2004), which encodes a requisite subunit of an odorant-gated ion channel (Sato et al., 2008; Wicher et al., 2008). Odorants bind discretely to OR proteins to create stereotyped neuronal responses (Yao et al., 2005; Hallem and Carlson, 2006).

The identification of transcription factors and promoter DNA binding sites that selectively control *Or* gene expression suggests that combinatorial transcriptional regulation underlies *Or* gene choice in *Drosophila* (Clyne et al., 1999; Ray et al., 2007, 2008; Tichy et al., 2008; Bai et al., 2009). Combinatorial regulatory activity might also underlie the expression of vertebrate class I *Or* genes (Hoppe et al., 2003, 2006). Yet how selective transcriptional mechanisms might account for the dispersed patterns of *Or* gene expression is unresolved.

The antenna was a subject of classical lineage studies that uncovered the compartmental organization of the *Drosophila* body plan (Morata and Lawrence, 1978, 1979). Mitotic clones induced after the formation of compartment borders remained contiguous in either of the antenna's two compartments. These studies relied on cuticle markers and did not fully resolve the behavior of sensilla beneath the epidermis. Here we show that olfactory sensilla are highly mobile and move considerable distances after their specification, though they respect the compartment boundary. The transcription factors Engrailed and Dachshund are redeployed to a spatially localized subset of sensillum progenitors, where they act as combinatorial determinants of sensillum identity and *Or* choice. Thus, it appears that, in *Drosophila*, the dispersed odorant receptor pattern can arise from the scattering of sensilla after the spatially defined determination of their *Or* identities.

## RESULTS

### Olfactory Sensilla Move beneath the Epidermis

The *Drosophila* olfactory apparatus consists of bilaterally symmetric antennae and maxillary palps that harbor approximately 1,200 and 120 ORNs, respectively (Figure 1A). The ORNs are organized into sensillum units containing 1–4 neurons and additional support cells. Each ORN sends an axon into the brain to synapse with the clustered dendrites of projection neurons (PNs) in morphological units known as glomeruli (reviewed by Davis, 2005; Figure S2 available online). The adult

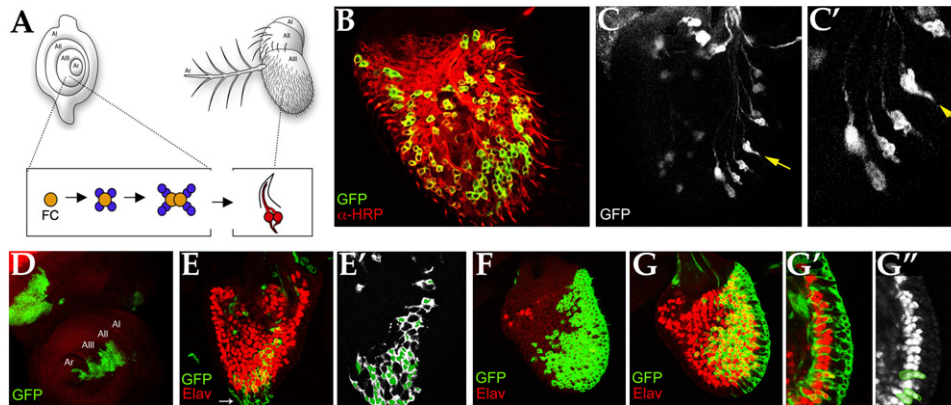


**Figure 1. Dispersal of Clonally Labeled Sensilla on the Olfactory Epithelium**

(A) An olfactory sensillum arises in the third segment of the antennal disk (AIII, top left) when a sensillum founding cell (FC) locally recruits precursors (blue) into a nascent cluster (bottom). Cell division expands the number of cells, which form a sensillum consisting of 1–4 neurons (red) and support cells in the mature third antennal segment (top right).

(B) A somatic mosaic clone induced in the third instar antennal imaginal disk was observed in the late pupal stage after sensilla have formed. Infrequent clones were induced by MARCM, with neuronal labeling by *elav-GAL4 > UAS-CD8::GFP* (green). All neurons were labeled by anti-HRP staining (red). GFP-labeled sensillum clusters are dispersed over a large area.

(C and C') Labeled sensillum ORN clusters (as in B) are dispersed along the proximal-distal axis (distal at bottom), interspersed with unlabeled sensilla. The dendritic membranes of sensillum ORNs coalesce at their apical tips (yellow arrows). Higher magnification of (C) is shown in (C').

(D) A MARCM clone (labeled by *tub $\alpha_1$ -GAL4 > UAS-CD8::GFP*) in the prospective third antennal segment (AIII) during the late third larval stage. Labeled cells at this stage are contiguous.

(E and E') A MARCM clone labeled with *tub $\alpha_1$ -GAL4 > UAS-CD8::GFP* in the early pupal stage (36 hr APF), shortly after disc eversion. Membrane-targeted CD8::GFP labeled cells (green in E; white/green in E') are interspersed with unlabeled cells (in E, neurons are labeled by anti-Elav, red color). A white arrow indicates contiguously labeled epidermal cells. Cytoplasmic fluorescence was used to identify GFP-positive cells (green color in E') since GFP-labeled membrane often enveloped nearby GFP-negative cells.

(F–G'') Confocal images spanning the anterior, posterior axis of a MARCM clone in a late-pupal-stage specimen. Cells were labeled with *tub $\alpha_1$ -GAL4 > UAS-CD8::GFP*. A superficial plane (F) reveals contiguous GFP (green) labeling of epidermis. A deeper plane (G) reveals GFP-labeled sensillum units interspersed with unlabeled sensilla (neurons labeled with anti-Elav, red color). A horizontal view at the edge of the epithelium (G' and G'') shows GFP-negative sensilla beneath GFP-positive epidermis. In (G''), GFP-positive sensilla are green and neurons (anti-Elav) are grayscale.

antenna arises from the eye-antennal imaginal disk, an epithelial sheet of concentric ring-like domains (Figure 1A) whose growth and patterning in the larva sets the stage for ORN differentiation in the pupa. The ORNs are thought to arise in a temporal process like ommatidial assembly in the compound eye (Ray and Rodrigues, 1995). This process begins with the appearance of founding cells (FCs; Figure 1A; Reddy et al., 1997) that arise in stereotyped locations and temporal sequence in the early pupal stage. An FC recruits adjacent cells into nascent sensillum clusters. A final cell division precedes the differentiation of sensillum cell types.

As a first step toward understanding lineage relationships in sensillum development, we examined somatic clones that labeled multiple sensilla. Mosaics were induced at several times during imaginal disc cell division during the larval stage. We used *FLP*-mediated interchromosomal recombination and positive fluorescent protein labeling (mosaic analysis with a repressible cell marker [MARCM]; Lee and Luo, 1999) or intrachromosomal recombination with “*flipout*” *GAL4* and *lacZ* reporter transgenes (Pignoni and Zipursky, 1997; Struhl and Basler, 1993). Both approaches produced heritable and stable *GFP* or *lacZ* expression and were calibrated to yield less than one clone per antenna, on average (see Supplemental Experimental Procedures; Figure 1D). Since late-larval-stage specimens with multiple antennal clones were rare, the distribution of labeled cells in an older specimen should usually reflect the behavior of a single clone.

When clones were induced in larval-stage animals and examined at the late pupal stage, GFP-positive ORNs were dispersed throughout the antenna, markedly intermixed with unlabeled neurons (59 specimens). Labeled neurons were often distributed over the entire length and/or width of the tissue (Figure 1B; 32/59 specimens). However, single labeled neurons were infrequent, as labeled neurons usually appeared in clusters of two or three (Figures 1C, 1C', and 2A) that evidently belonged to a single sensillum. Their dendrites, labeled by membrane-targeted GFP, coalesced into bundles entering single bristles (arrows in Figures 1C and 1C'). When MARCM was performed with the ubiquitous *Tubulin $\alpha_1$ -GAL4* driver, all cell types, including neurons, support and epidermal cells, were colabeled within a single clone (Figures 1F and 1G; Figure 5E). Clonally derived epidermal cells (Figure 1F; 33 specimens) typically formed a relatively contiguous patch that overlaid labeled and unlabeled sensilla (Figure 1G). Thus, sensilla and epidermal cells behaved differently, with labeled sensilla interspersed with unlabeled sensilla below contiguously labeled epidermis.

To define the temporal period in which the separation and intermixing of lineally related ORNs occurred, clones were induced at the midlarval stage (72 hr–96 hr after egg laying [AEL]) and examined at several time points through midpupation, a range encompassing most of sensillum development. Clonal cells were contiguous prior to the pupal stage (29 specimens; Figure 1D). The dispersal of clonally related neuronal cell clusters

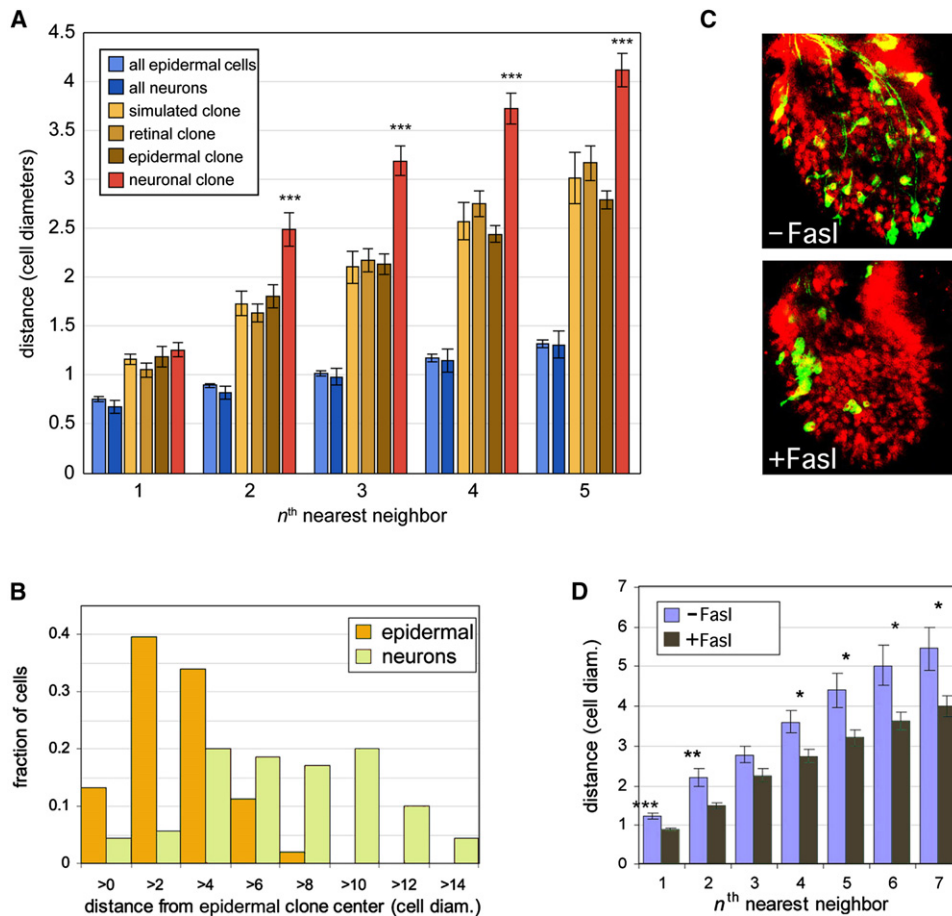


**Figure 2. Statistical Analysis of Clonal Cell Distributions in the Antenna**

(A) Nearest neighbor analysis of clonally related cells. The average distance (in cell diameters) was compared between colabeled cells in neuronal, epidermal, retinal, and “simulated” clones (see Supplemental Experimental Procedures). Distances between cells of a given cell type were normalized by the average distance between adjacent (nonclonal) cells of the same cell type. Statistical significance is indicated (\* $p < 0.05$ ; \*\* $p < 0.01$ ; \*\*\* $p < 0.001$ ).

(B) Distance of clonal cells from the geometric center of a clone. A clone center was computed on the basis of the X, Y coordinate location of all labeled epidermal cells when GFP-labeled clones were generated with *tub > y<sup>+</sup>, CD2 > GAL4; UAS-CD8::GFP*. The fraction of cells (neuron or epidermal) more than a particular distance (in cell diameters) is indicated. Labeled epidermal cells were closer to the geometric center of the clone than neurons.

(C) Typical specimens, bearing GFP-labeled clones as in (B), with or without *UAS-fas1<sup>+</sup>* expression. GFP-positive neurons were clustered when they expressed FasI (bottom).

(D) Nearest neighbor analysis of clonally labeled neurons, with and without ectopic expression of FasI. Statistical significance is as in (A).

was first evident in the second pupal day (22 specimens; Figure 1E, arrow indicates labeled epidermis). Intercluster distances increased over a period of 36 hr. Notably, this period of neuronal dispersal followed soon after the early events of sensillum development.

These qualitative observations suggested that young sensilla become mobile soon after their initial development. To quantify the spatial relationships between the cells of a clone, we analyzed the pair-wise distances between labeled cells in mid-pupal-stage specimens (Figures 2A and 2B). Each antennal specimen was imaged as a three-dimensional stack of confocal micrographs so that the distance of each labeled neuron or epidermal cell to all other labeled cells (neuron or epidermal) could be calculated, normalized, and ranked (see Supplemental Experimental Procedures). As shown in Figure 2A, the labeled neuron nearest to a labeled neuron ( $n = 1$ ) was about 1.3 cell

diameters away, as labeled neurons were often found in pairs within a sensillum (e.g., Figure 1C). In contrast, a disproportionately larger gap separated a labeled neuron from the second, third, or fourth distal-labeled neurons. Clonally labeled epidermal cells, on the other hand, were distributed evenly with respect to rank (Figure 2A). The fourth nearest neuron to a labeled neuron was nearly 1.5 cell diameters further than the distance between labeled epidermal cells of the same rank. In addition, the geometric center of all labeled neurons was shifted away from the center of labeled epidermal cells belonging to the same clone (Figure 2B), such that labeled neurons were shifted beneath unlabeled epidermis. Finally, clonally labeled neurons spread over a significantly larger radial distance than did epidermal cells (Figure 2B).

We considered two models for the dispersal of clonally related cells to compare statistically with the behavior of ORNs. In the

first, clonally labeled cells were examined in the retina, where some cell movement and clonal mixing occurs over short distances as precursors join ommatidial cell clusters (Ready et al., 1976; Lawrence and Green, 1979). For retinal clones, the distance between each labeled  $n^{\text{th}}$  neighbor was found to increase by a constant  $\sim 0.5$  cell diameter, well below the increment observed for olfactory neurons (Figure 2A). A second model for cell movement during proliferation was developed theoretically and simulated *in silico* (Supplemental Experimental Procedures; Movies S1 and S2). The positions of hundreds of cells in a bounded square plane were computed as each cell progressed through cycles of cell division. As new cells were generated by cleavage in a random direction within the sheet, the cell arrangements were continuously “relaxed” to minimize the proximity of each cell’s center to those of its neighbors (Movie S1). This simulated cell displacement resulted in dispersal similar to that observed experimentally in the retina and for antennal epidermal cells (Figure 2A). The behavior of clonally related cells in both of these models was distinct from that of olfactory receptor neurons.

As a test of the notion that clonally related neurons originate in close proximity, we examined the effect of inhibiting dispersal by ectopically expressing the homophilic cell adhesion molecule Fasciclin I (Zinn et al., 1988) within clones. Fasciclin I promotes the association of cells and cellular appendages in both cell culture and *in vivo* (Elkins et al., 1990). Rare FRT recombination events were used to induce *GAL4* expression and transactivate *UAS-fasciclin I* and *UAS-CD8::GFP* during the expansion of a clone (Figure 2C). Spatial analysis of cell position (Figure 2D) revealed that neurons expressing Fasciclin I are tightly clustered. These observations suggest that enhanced homophilic adhesion prevents the migratory separation of sensilla, which remain together near their clonal origin.

### A Switch in the Expression of the Posterior Determinant Engrailed

The antenna is composed of posterior and anterior compartments, as defined by a clonal analysis employing cuticular markers (Morata and Lawrence, 1979). It is unclear, however, whether neurons and other sensillum components beneath the epidermis respect compartmental restrictions; at least one sensory structure, the “bristle of doubt,” can escape compartmentalization (Morata and Lawrence, 1979). Posterior compartment cells are marked by the expression of Engrailed (En), a determinant of posterior identity (Morata and Lawrence, 1975). Cells lacking *en*<sup>+</sup> function, for example, in *en*<sup>-</sup> somatic clones, can be extruded from posterior epithelia (Kornberg, 1981; Lawrence and Struhl, 1982). As we describe below,  $\sim 25$  olfactory sensilla in the anterior compartment are primarily composed of En-positive cells, whereas  $\sim 45$  sensilla in the posterior compartment lack En expression. For the most part, anterior En-positive sensilla and posterior En-negative sensilla reside in their compartments of origin. Thus, a large fraction of sensilla switch their state of Engrailed expression early in their development.

Engrailed (En) expression was examined in the developing and mature antenna with three well-characterized antibody and transgenic reagents (anti-mAb4D9, *P{en-lacZ}en<sup>Xho25</sup>* and *P{en2.4-GAL4}en<sup>16E</sup>*). In the larva and early pupa, Engrailed was

expressed uniformly in the posterior compartment and absent from the anterior compartment of the antennal disk (Figures 3A and 3B). However, by 7 hr after puparium formation (APF), En expression was detected in a few anterior compartment cells (Figure 3C) and reduced or undetectable in many posterior compartment cells (arrowheads, Figure 3C'). By 9 hr APF, there were 11–14 En-positive cells in the anterior compartment, which were roughly aligned in a crescent (arrow in Figure 3F). These En-positive cells were identified as sensillum (FCs), which arise in three semicircular domains at this stage (Figures 3G, 3E, and 3E'; Ray and Rodrigues, 1995; Reddy et al., 1997). By 16 hr APF, disk eversion transforms the flat antennal imaginal disk into the segmented tubular adult appendage (Figure 4A). The anterior compartment En-positive sensilla were observed in an irregular pattern at this (24 hr APF; Figure 3H) and later times (Figures 4B, 4E, and 4H). In the posterior compartment (Figures 4C and 4D), En-positive and En-negative sensillum clusters were distributed in alternating stripes at early pupal time points (Figure 4D'). The stripe pattern was absent in older specimens (Figure 4F; third pupal day).

A redefinition of expression pattern likewise occurred for Dachshund (Dac), a transcription factor that, like Engrailed, has an early role in imaginal disk development (Mardon et al., 1994; Lecuit and Cohen, 1997). Dac was expressed in a contiguous horseshoe pattern straddling the anterior-posterior compartment border in the larval antennal disk (Figure 3D; Mardon et al., 1994). The Dac-positive cell population intersected the En-positive cell population such that some FCs expressed both genes (Figures 3D and 3D', inset). By the second pupal day ( $\sim 36$  hr APF; Figure 4G), Dac-positive cells were distributed broadly, interspersed with Dac-negative cells and included in the two possible classes with respect to Engrailed expression (Figures 4G–4I).

Given the evident mobility of young sensilla, we considered whether movement across the compartment border might account for the presence of En-positive sensilla in the anterior compartment and En-negative sensilla in the posterior compartment. Single progenitor clones and En expression were visualized after sensillum formation and dispersal (Figures 5C–5E). Labeled clones containing En-positive neurons in the anterior compartment always included En-negative neurons (21 specimens). Similarly, En-positive and En-negative neurons shared labeled clones within posterior territory (18 specimens). There was little evident movement of anterior or posterior derived cells across the compartment border, only an occasional intrusion consistent with local mixing (arrow in Figure 5D). Similarly, in both compartments, single progenitor clones harbored both Dac-positive and Dac-negative ORNs (12 specimens; Figures 5F and 5G) and were also mixed for the expression of En (12 specimens). Thus, we suppose that sensillum progenitors switch their state of En and Dac expression early in sensillum development.

Since many cells alter their state of En and/or Dac expression prior to or during sensillum formation, it was unclear whether subsequent changes in the pattern of En and Dac were due to additional alterations in cellular expression or identity, or attributable instead to stable expression in cells that disperse. We therefore utilized the photo-switchable fluorescent protein Kaede (Ando et al., 2002) to mark cells *in vivo* (Figures 5A and

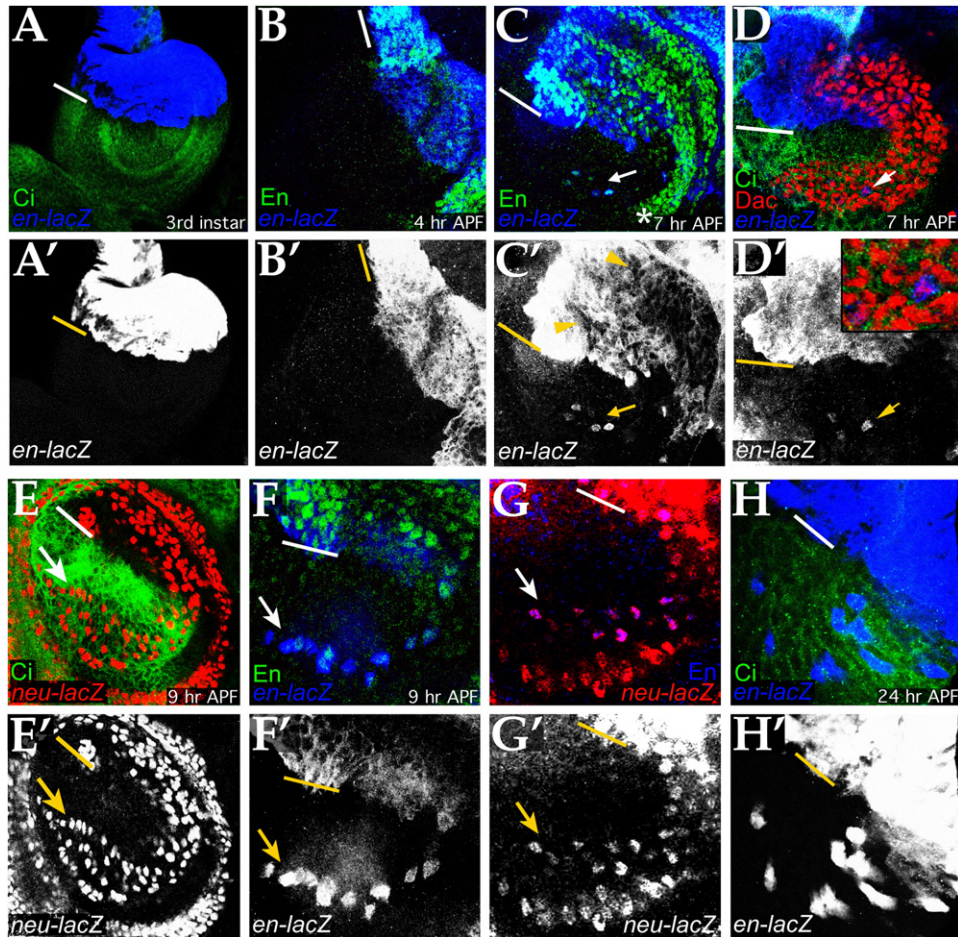


**Figure 3. Engrailed Is Redeployed in Young, Developing Sensilla**

(A–D) *engrailed* expression in late larval and early pupal stage. In the larva (A; third instar), *engrailed* (*en-lacZ*; anti- $\beta$ -galactosidase, blue color; grayscale in A') is expressed uniformly in the posterior compartment. *Ci* is expressed in the anterior compartment (anti-*Ci*, green color; compartment border indicated by white line). A similar pattern is found at the beginning of the pupal stage (B), 4 hr APF; *en-lacZ*, blue color; anti-En antibody, green color. A few hours later (C), 7 hr APF; staining as in (B), En-positive cells are detected in the anterior compartment (arrow), and posterior compartment cells display reduced or no En expression (arrowheads in C'). Dachshund-positive cells D (anti-Dac, red color) form a horseshoe spanning the compartment border. Some Dac-positive cells are Engrailed-positive (arrows; high magnification inset in D', *en-lacZ* reporter, blue color, shown alone in D'). Anti-*Ci* (green color) marks the anterior compartment.

(E–H) Engrailed is expressed by sensillum founding cells (FCs). At early pupal stage (E; 9 hr APF), the FCs arise in semicircular domains (yellow arrow; marked by *neu-lacZ*, red color in E; grayscale in E'). En-positive cells arrayed in a semicircular domain at 9 hr APF (F; *en-lacZ*, blue color, grayscale in F') are coincidentally labeled by *neu-lacZ* (G), anti-mAb4D9, blue color; anti- $\beta$ -galactosidase, red color, grayscale in G'). By 24 hr APF, En-positive FCs have dispersed (*en-lacZ*, blue color in H; grayscale in H'). Anti-*Ci* (green color) labels the anterior compartment in (E) and (H). A solid line marks the compartment border in all panels.

5B). Animals expressing Kaede in En-positive cells (*en-GAL4* > *UAS-Kaede*) were exposed to violet light at time points during the first pupal day and examined for the perdurance of red fluorescence at the beginning of the second pupal day. Thus, in these experiments, cells that expressed En after violet light exposure are marked by Kaede in its native state (green), whereas cells that expressed En prior to violet light exposure are marked by photo-switched Kaede (red). Notably, with switching at 12 hr APF, when En-positive FCs are still arrayed in a spatially stereotyped pattern (Figure 3F), nearly all green Kaede fluorescent cells at 24 hr APF (i.e., after dispersal) displayed red fluorescence (Figure 5B). All red fluorescent cells displayed green fluorescence (Figure 5B; data not shown). In contrast, red fluorescent cells were absent from the anterior

compartment when photo-switching was done before the appearance of En-positive FCs. We conclude that cellular En expression is dynamic prior to sensillum formation, but is stable thereafter; later changes in En distribution are therefore attributable to cell dispersal, not to labile En expression. Thus, as observed with clonally marked cells (Figures 1 and 2), En-positive sensilla appear to become motile, disrupting an early spatially stereotyped pattern.

#### ***engrailed* and *dachshund* Expression Are Precisely Correlated with Sensillum Identity and *Or* Gene Expression**

Since clonally related sensilla were distributed across the epithelium in a manner similar to patterns of *Or* gene expression, we

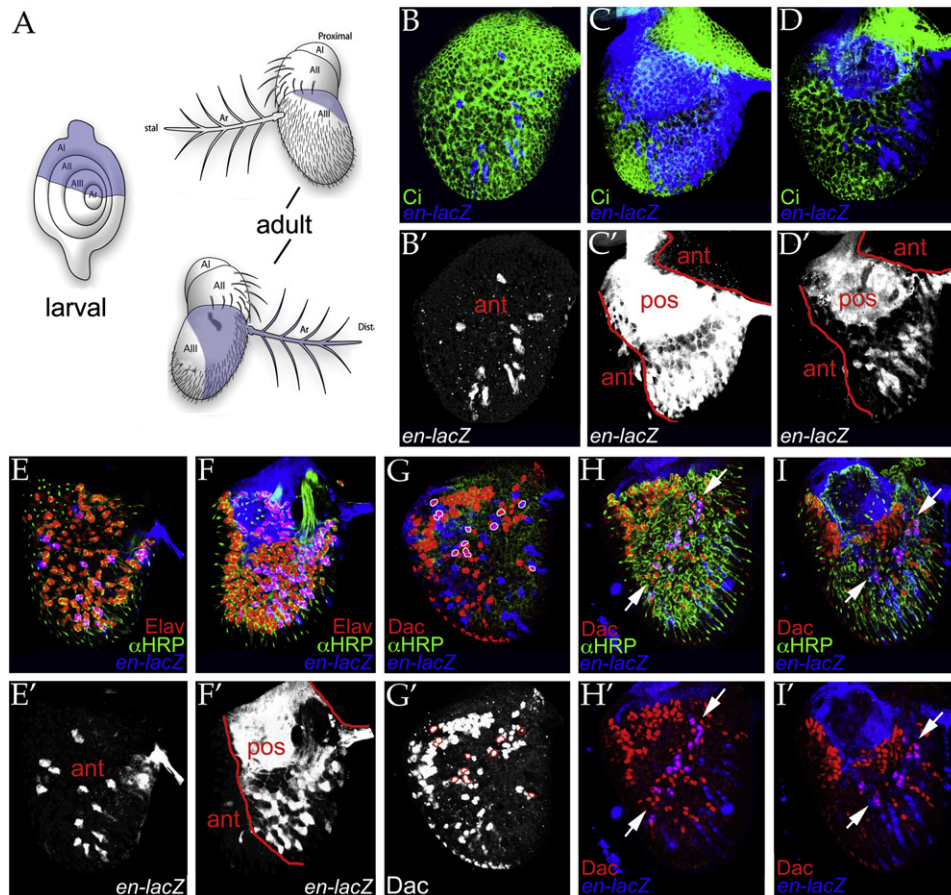


**Figure 4. Sensillum Identities Defined by En and Dac Expression**

(A) Compartments of the larval and adult antenna. Eversion at the end of the first pupal day transforms the flat imaginal disc (left) into a segmented pouch, the precursor to the adult antenna (right top, bottom). The proximal-distal locations of the four antennal segments (AI–AIII, Ar) and their larval primordia are indicated. Anterior and posterior compartments are labeled (posterior, purple shading). Opposing perspectives are shown on the right, top and bottom, for the adult antenna.

(B–D) En-positive sensilla in the early postembryonic antenna. En-positive sensilla are visualized at 24 hr APF (*en-lacZ*, blue color in B–D; grayscale in B'–D'); anti-Ci, green color) in the anterior (B, B'), and posterior compartments (D, D'). Posterior compartment epidermis is uniformly En-positive (C, C'). Red lines indicate the anterior (ant), posterior (pos) borders in (C') and (D').

(E–F) En-positive sensilla in midpupal stage. En-positive sensilla (*en-lacZ*, blue in E, F; grayscale in E', F') were visualized at 48 hr APF in the anterior (ant, E) and posterior (pos, F) compartments. All neurons are stained with anti-Elav (red color) and anti-HRP (green color).

(G–I) Dac expression in En-positive and En-negative olfactory neurons. Mid- (G) and late- (H, I) pupal-stage specimens were labeled for Dac (anti-Dac, red color) and En (*en-lacZ*, blue color) expression. A subset of olfactory neurons in the anterior (G, H) and posterior (I) compartments expresses both Dac and En (circled in G, G'; region between arrows in H–I). All neurons are labeled by anti-HRP (green color) in (H) and (I).

asked whether ORNs that express the same *Or* gene share a close lineage relationship. Neurons belonging to small, labeled clones were examined to determine if they often express the same *Or* gene (Figure S1A). We also asked whether the axons of ORNs belonging to a small clone targeted the same antennal lobe glomeruli, which would be the case for ORNs expressing the same *Or* gene (Figures S1B and S1C; see Davis, 2005). Neither approach revealed a close linkage between clonal origin and *Or* gene expression.

We then considered whether Engrailed and Dachshund are linked to the expression of specific *Or* genes. *Or* genes are expressed in stereotyped combinations in defined sensillum types (Figure 6; Dobritsa et al., 2003; Elmore et al., 2003; Hallem et al., 2004; Goldman et al., 2005; Couto et al., 2005; Fishilevich and

Vosshall, 2005). The antennal ab4 sensillum contains two neurons that, respectively, express *Or56a* and *Or7a*. These ORNs were always En-positive (Figure 6). The two neurons of sensillum ab8 express *Or9a* and *Or43b* respectively; these ORNs were also En-positive. The at3 sensillum was shared by two En-positive neurons, expressing *Or2a* and *Or19a*, respectively, and one En-negative (*Or43a*-positive) neuron. In total, four sensillum types contained neurons that were En-positive and Dac-negative. Another seven sensillum types (ab1, ab3, ab7, ab9, ab10, pb1, and pb3) contained En-negative and Dac-positive neurons. Three of these sensilla (ab1, ab3, and ab7) contained both Dac-positive and Dac-negative neurons. Thus, like En, Dac expression was strictly correlated with the expression of specific *Or* genes (Figure 6). The two ORNs of

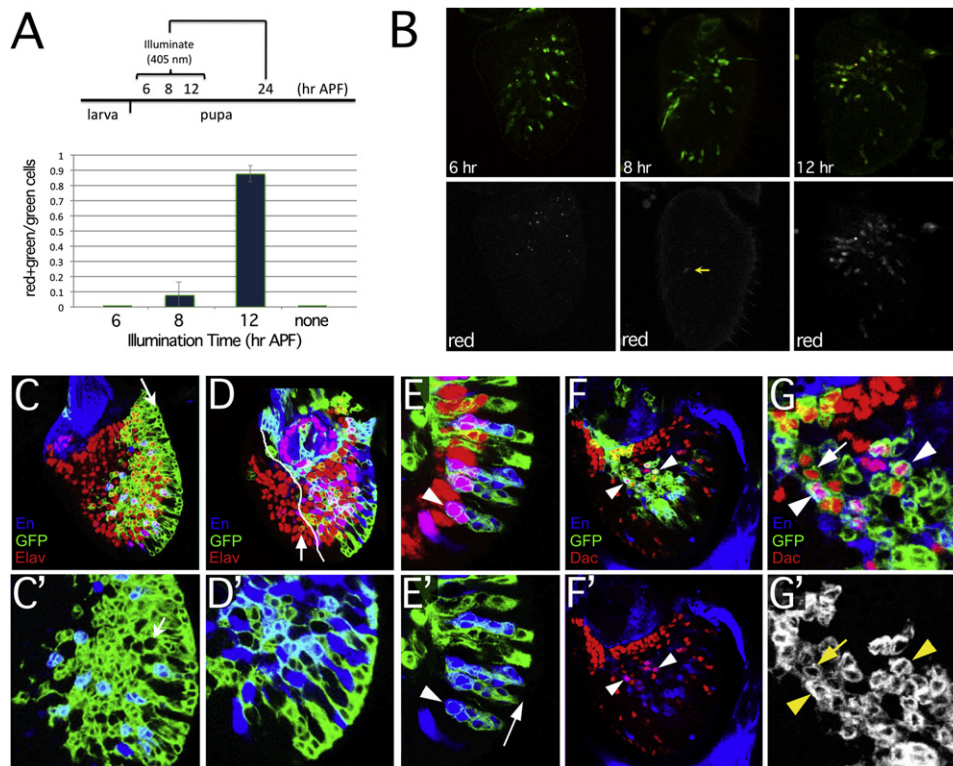


### Figure 5. A Switch in Compartmental Expression of Engrailed

(A and B) Tracing En-positive neurons in the anterior compartment with photo-switchable Kaede protein. Intact pupal stage *en-GAL > UAS-Kaede* animals were exposed violet light (100 W Hg lamp/ peak 405 nm) for 2 min at the indicated time points (A, top) to convert Kaede to the red fluorescent isoform. Antennae were isolated at ~24 hr APF and examined for green and red fluorescence (B). Red and green fluorescence is shown in (B), top panels. Red fluorescence is shown alone in (B), bottom panels. Nearly all green fluorescent cells displayed red fluorescence after illumination at 12 hr APF but not with illumination at the earlier time points (A). Error bars indicate SEM.

(C–E) Infrequent MARCM clones labeled with *tub $\alpha_1$ -GAL4 > CD8::GFP* (green color) were induced at the second instar and examined in late pupal stage specimens. *engrailed* was monitored with *en-lacZ* (blue color) and neurons were labeled with anti-Elav (red color). In (C), a large clone in the anterior compartment includes both En-positive and En-negative sensilla. An arrow indicates contiguously GFP-positive epidermis in the plane on the edge of the specimen. A higher magnification view of the same specimen (C') reveals a GFP-negative sensillum surrounded by GFP-positive sensilla (arrow). In (D) (higher magnification in D'), a posterior clone displays considerable intermixing of GFP-positive and GFP-negative sensilla. A white line marks the compartment boundary in (D); anterior is to the left. In (E), MARCM labeled sensillum cell clusters are shown at high magnification beneath unlabeled epidermis (arrow in E'). Note that clones include most or all cells of a sensillum, including both neurons (anti-Elav, red color) and support cells.

(F and G) Clonal analysis of Dac-positive cells. Dac-positive (anti-Dac, red color) and En-positive (*en-lacZ*, blue color) cells were labeled by GFP (green in F, G, grayscale in G') in MARCM clones. In (F), a clone in the posterior compartment at early pupal stage contains cells in all four possible classes with respect to En and Dac expression. Arrowheads indicate En-positive and Dac-positive neurons. A higher magnification view of this clone is shown in (G) and (G').

maxillary palp sensillum pb2 were En-positive and Dac-positive. *Or13a*, which has not been assigned to a sensillum, was also found only in En-positive and Dac-positive ORNs. The remaining five defined sensillum types expressed neither En nor Dac. Notably, En and Dac expression was not correlated with particular sensillum morphological types (e.g., basiconic, trichoid, or coeloconic).

The axons of ORNs target first-order projection neurons in a spatially stereotyped ensemble of 43 glomeruli in the brain's antennal lobe neuropil. ORNs that express the same *Or* gene send their axons to the same glomerulus (reviewed in Davis, 2005). The axonal projection pattern of En-positive ORNs has previously been examined via the use of the *en-GAL4* driver and a marker for axonal termini, *UAS-nSynaptobrevin::GFP* (*nSyb::GFP*; Blagburn, 2008; Chou et al., 2010). We also examined these axonal projections. Nineteen glomeruli were strongly

labeled (Figure S2; Table S1), a pattern which agreed, to a first approximation, with the expectation based on *Or* gene expression (Couto et al., 2005; Fishilevich and Vosshall, 2005). There were a few notable exceptions. Though the *Or43a* ORNs were not detectably En-positive (Figure 6), the *Or43a*-targeted glomerulus, DA41, was labeled by En-positive axons. We note that the *Or43a* ORN shares the at3 sensillum with two En-positive ORNs and *Or43a* expression is *engrailed*-dependent (below; Figure S3B). *Or47a* and *Or82a* formed another anomalous pair, expressed in two ORNs in the ab5 sensillum. Both ORNs appeared En-negative, but their respective target glomeruli were labeled by *en-GAL4* driven axonal reporter expression. The expression of these *Or* genes also displayed *en*<sup>+</sup> dependence (below). We suspect that these ORNs may be transiently En-positive and/or have expressed En at an undetected level.

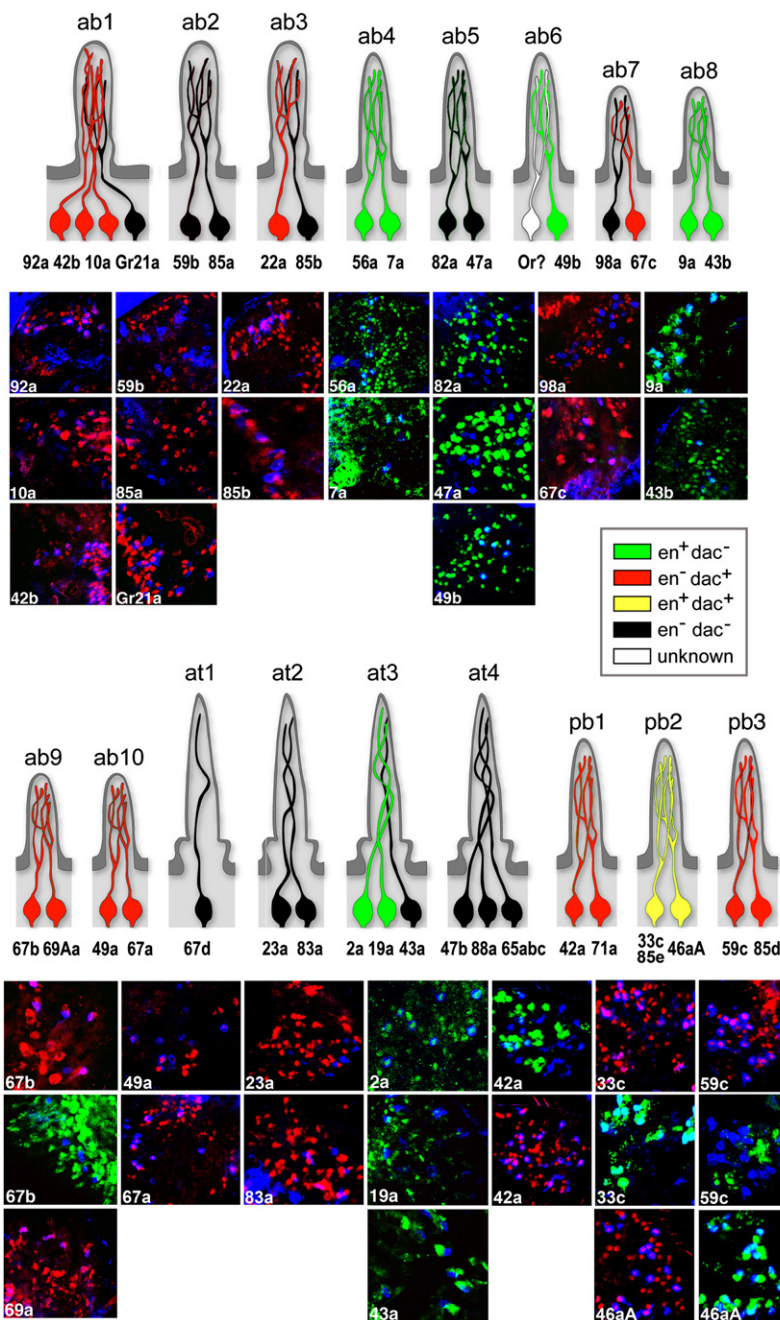


**Figure 6. Coupling of En and Dac Expression to odorant receptor and Sensillum Identity**

Seventeen identified sensillum types in the antenna and maxillary palp are depicted schematically, with odorant receptor expression and morphological class indicated. The micrographs (bottom panels) show neurons labeled for expression of the indicated *Or* gene (blue color; see Table S1) and En (green color, *en-lacZ* or anti-En) or Dac (red color, anti-Dac). The schematic labels each neuron in accordance with En and Dac expression:  $En^+ Dac^+$  (yellow),  $En^+, Dac^-$  (green),  $En, Dac^+$  (red), and  $En^-, Dac^-$  (black). No color indicates that the *Or* is unknown.

***engrailed* and *dachshund* Are Selectively Required for *Or* Gene Expression**

Given the coincident expression of Dac and En with specific *Or* genes, we next considered whether *dac+* and/or *en+* might be required for *Or* expression. Both *en+* and *dac+* have essential early patterning roles, so we employed hypomorphic alleles that display normal antenna development and transgenic gain and loss-of-function alleles that permitted temporal and spatial control of wild-type activity.

Animals heterozygous for *dac<sup>1</sup>/dac<sup>9</sup>* develop normally to adulthood with relatively normal antennae (Figure 7A; data not shown). When examined with *Or* reporters (Figure 7A) or by RT-PCR (Figure 7B), the expression of most Dac-positive *Or* genes was selectively reduced (*Or13a*, *Or22a*, *Or42b*, *Or46a*, *Or49a*, *Or67a*, *Or67b*, *Or67c*, *Or69aA*, and *Or92a*). *Or* expression was nearly undetectable in three cases (*Or13a*, *Or67b*, and *Or92a*), whereas in two cases the reduction was small but significant (*Or46a* and *Or67c*). In one case, *Or42a*, a small apparent decrease was not statistically significant. Similar results were obtained by eliminating *dac+* via temporally controlled RNA interference (RNAi). Here, a *UAS-dac<sup>hpn</sup>* transgene was expressed in the pattern of *dac+* with *dac-GAL4* and temporally restricted to ORN development with temperature-sensitive *GAL80<sup>ts</sup>* (Figure 7A, bottom). The variable loss of *Or* expression observed with these approaches might reflect differing thresholds

The axonal projection pattern of Dac-positive ORNs was similarly examined by using *dac-GAL4* to label axon termini with nSyb::GFP. This selectively labeled 22 glomeruli, which were as predicted on the basis of *Or* gene expression in Dac-positive ORNs (Figure S2; Table S1). Three glomeruli were coincidentally labeled by *en-GAL4* and *dac-GAL4*, also as predicted by *Or* gene expression. Two of these glomeruli (VA7I and VC1) were targeted by the En-positive, Dac-positive ORNs of the pb2 sensillum, which express *Or46a* and *Or33c/Or85e*, respectively. Another glomerulus, DC2, was targeted by the *Or13a*-positive ORNs. The identity of the ORNs targeting the En-positive, Dac-positive VA7m glomerulus is unknown.

for the *dac+* requirement or variance in residual *dac+* activity. In contrast, *Or* genes expressed in Dac-negative ORNs were not affected by *dac* loss-of-function (Figures 7A and 7B; *Or33a*, *Or43b*, *Or47b* [data not shown], *Or56a*, *Or59b*, and *Or85a*). One notable exception was the significant reduction of *Or98a*-positive neurons (Figure 7A) and the level of *Or98a* mRNA (Figure 7B). Notably, the Dac-negative *Or98a* neuron shares a sensillum with the Dac-positive *Or67c*-positive neuron; it might have been transiently Dac-positive, or *Or98a* expression might depend on the *Or67c*-positive neighbor. Thus, with minor exceptions, *dac+* function was selectively required in Dac-positive ORNs for normal *Or* gene expression.

We likewise examined the requirement for *en*<sup>+</sup> in *Or* gene expression, employing the viable *engrailed* mutants *en*<sup>1</sup> and *en*<sup>54</sup>, in addition to spatially and temporally controlled RNAi (Figure 7B; Figures S3A and S3B). The expression of most *Or* genes in En-positive ORNs was significantly reduced in *en* loss-of-function animals (*Or2a*, *Or7a*, *Or9a*, *Or19a*, *Or33c*, *Or43a*, *Or43b*, and *Or56a*) with the exception of three cases (*Or13a*, *Or46a*, and *Or49b*). However, there also were significant losses of En-negative *Or22a* and *Or69a* neurons. We considered, as a possible explanation, that the *en* alleles affected posterior compartment patterning prior to sensillum development; notably, *Or69a*-positive ORNs were exclusively located in the posterior compartment. To circumvent this problem, RNAi was restricted to the anterior compartment, using *cubitus interruptus* (*ci*)-GAL4 to drive *UAS-en*<sup>hpn</sup>. These animals were adult-viable and morphologically normal; in contrast, driving *UAS-en*<sup>hpn</sup> in the posterior compartment with *en*-GAL4 was lethal. As shown in Figure 7C, the frequency of En-positive ORNs (*Or2a*, *Or19a*, *Or43a*, *Or46a*, and *Or56a*) was significantly reduced in the anterior compartment, but essentially unchanged in the posterior compartment (Figure 7C, top). Moreover, En-positive *Or* genes expressed only in the posterior compartment were not affected (*Or9a*, *Or13a*, *Or43b*, and *Or49b*). To resolve this requirement for *en*<sup>+</sup> function temporally, we placed *ci*-GAL4 driven *UAS-en*<sup>hpn</sup> under *GAL80*<sup>ts</sup> control. The number of *Or56a*-positive neurons was strongly reduced when *GAL80*<sup>ts</sup> was inactivated at the onset of pupation, which eliminated anterior compartment En expression during the first pupal day (Figure 7C, bottom; data not shown). In contrast, later onset of *en* RNAi resulted in a much smaller, though significant, reduction in *Or56a* expression. Thus, *en*<sup>+</sup> function is required in the first pupal day, when En-positive FCs were first detected in the anterior compartment (Figure 3).

To ask whether the requirements for *en*<sup>+</sup> and *dac*<sup>+</sup> are cell autonomous, we examined *en* or *dac* loss-of-function in mosaic animal. Mosaics were produced via *FLP* recombinase mediated loss of a *GAL80* transgene, which permitted *GAL4* transactivated expression of RNAi-inducing “hairpin” constructs. For targeting *en*, we used *en*-GAL4 to drive *UAS-en*<sup>hpn</sup> and *dac*-GAL4 was used to drive *UAS-dac*<sup>hpn</sup> expression. A *UAS-mCherry* reporter was included to fluorescently mark cells with active *GAL4*. (Figure S3C; Supplemental Experimental Procedures). Recombinational loss of *GAL80* was induced just prior to sensillum development. We then asked whether En-positive or Dac-positive cells lacking *en*<sup>+</sup> or *dac*<sup>+</sup> function, respectively, had normal *Or* gene expression. Indeed, ORNs with *en* loss-of-function were less likely to express the En-positive *Or56a* or *Or2a* genes (Figures S3C and S3D; data not shown). Similarly, ORNs with *dac* loss-of-function were less likely to express the Dac-positive *Or22a* gene (Figure S3D). Given that only a small proportion of cells were included in RNAi-positive mosaic clones, these data indicate that *en*<sup>+</sup> and *dac*<sup>+</sup> act cell autonomously in *Or* gene expression.

### **engrailed Is an Instructive Determinant of Sensillum Identity**

Given that *en*<sup>+</sup> is selectively required for *Or* gene expression, we wondered whether it might also act instructively. Hence, we asked whether ectopic *en*<sup>+</sup> expression could induce En-positive ORN identities. The relative simplicity of the maxillary palp,

harboring only three sensillum types (pb1, pb2, and pb3), facilitated such an analysis (Tichy et al., 2008; Bai et al., 2009). The pb2 sensillum contains a pair of En-positive and Dac-positive ORNs, whereas pb1 and pb3 are En-negative and Dac-positive (Figure 6). The *dac*-GAL4 driver could thus be used to drive *UAS-en*<sup>+</sup> in all maxillary palp ORNs to ask whether *Or* genes normally expressed in pb2 would be induced in place of *Or* genes specific to the other two sensillum types. In these animals the average number of pb2-specific *Or46a*-positive ORNs increased by 2.5 fold (Figure 7D), whereas the number of pb1-specific *Or42a*-positive ORNs decreased by 7-fold. This suggested that the pb1 sensillum might be transformed to the pb2 identity. However, pb2 also harbors an ORN expressing *Or33c*. The number of *Or33c*-positive ORNs was unchanged in the presence of ectopic *en*<sup>+</sup> (Figure 7D). Rather, the induced *Or46a* ORNs appeared as adjacent pairs (Figure S3E). Thus, we suppose that ectopic *en*<sup>+</sup>, under the conditions of this experiment, produced only a partial transformation to pb2 identity.

Interestingly, *Pdm3* is expressed in the four En-negative pb1 and pb3 ORNs and not in pb2. Yet, despite this widespread expression, only *Or42a* expression is absent in *pdm3* mutant animals (Tichy et al., 2008), as was observed for ectopic *en*<sup>+</sup> expression above. We therefore asked whether *pdm3* expression is affected by ectopic *en*<sup>+</sup> expression. Indeed, *pdm3* expression was nearly eliminated by ectopic *en*<sup>+</sup> expression (Figure S3F). En thus appears to act upstream of *Pdm3* in the control of ORN identity.

### **DISCUSSION**

In most olfactory systems studied to date, ORNs express one or two *Or* genes selected from a large genomic pool. Neurons that express the same *Or* gene are dispersed across sensory epithelia, intermixed with neurons that express different *Or* genes. These dispersed patterns are roughly similar across individuals, with the expression of each *Or* gene restricted to a characteristic zone of epithelia. The mechanism(s) underlying the formation of these patterns is unclear. An oft-considered possibility is that stochastic processes select *Or* genes from regionally restricted palettes (reviewed in Fuss and Ray, 2009). Our data indicate that some *Or* identities in *Drosophila* are established in early spatially stereotyped patterns that are later disrupted by sensillum motility, scattering sensilla across characteristic domains. Thus, patterning by spatial positional determinants may be sufficient to explain the *Drosophila* odorant receptor pattern.

These conclusions are based, in part, on somatic mosaic analysis. Clonally labeled sensilla containing from one to four neurons and associated support cells were found many cell diameters away from their nearest labeled siblings in mature epithelia, intermixed with unlabeled sensilla (Figures 1 and 2). Labeled epidermis, in contrast, remained relatively contiguous (Figure 1G). The dispersal and intermixing of labeled and unlabeled sensilla began several hours after the onset of sensillum development (Figure 1) and appeared complete by late pupation. We could suppress sensillum dispersal by increasing intersensillum adhesion via the ectopic expression of a homotypic cell adhesion protein (Figures 2C and 2D). This suggests that clonally related sensilla arise in close proximity.

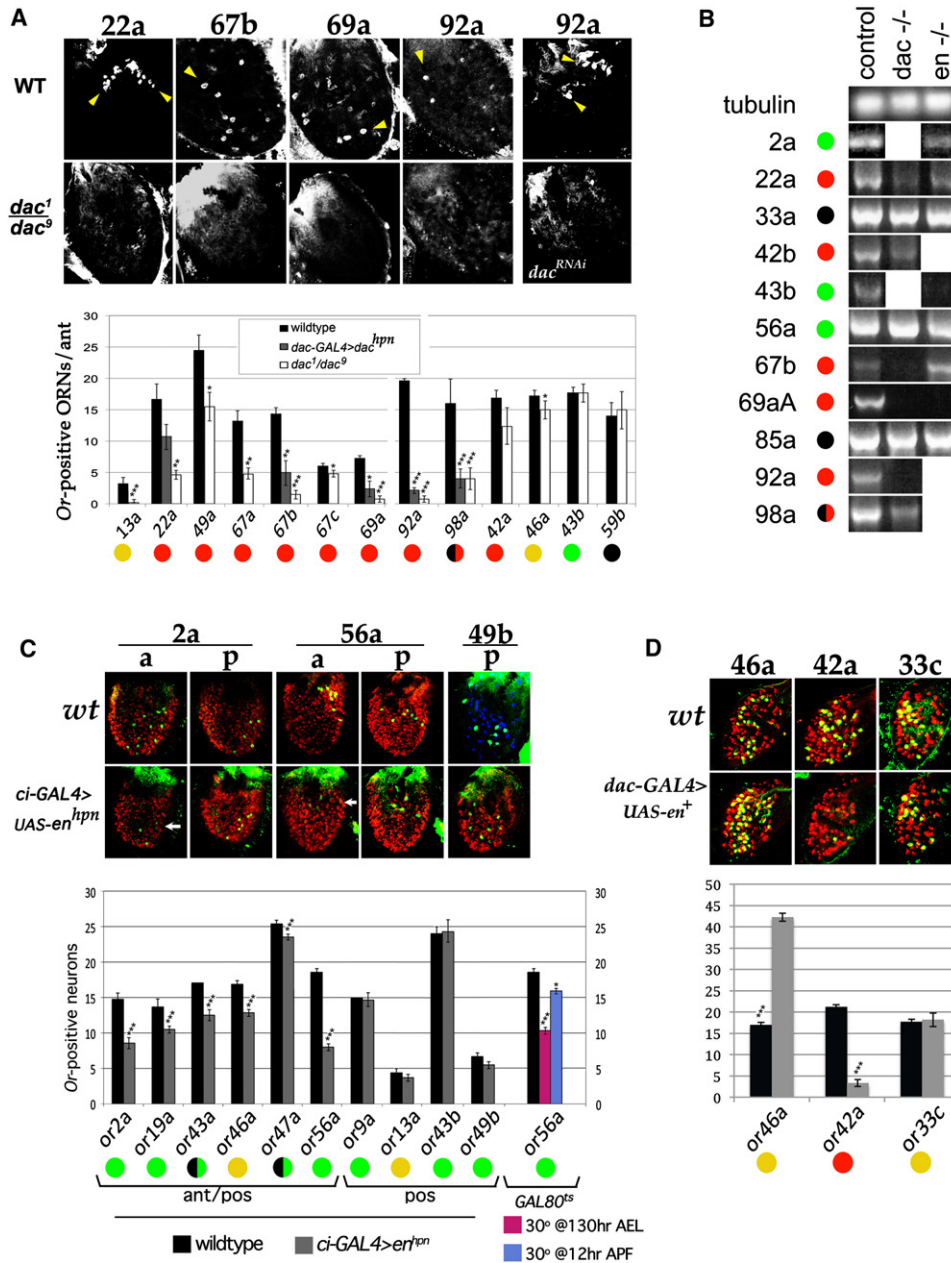


**Figure 7. En and Dac Are Determinants of Or Choice**

(A) *Or* gene expression requires *dac*<sup>+</sup> function in Dac-positive ORNs. Late pupal stage antennae from *dac<sup>1</sup>/dac<sup>9</sup>* heterozygotes and *dac-GAL4, UAS-dac<sup>hpn</sup>, tubα<sub>1</sub>-GAL80<sup>ts</sup>* animals were examined for expression of the indicated *Or* gene reporters (anti-GFP staining; grayscale, top micrograph panels). For RNAi induction, *GAL80<sup>ts</sup>* was inactivated by a temperature upshift (18°C to 30°C) at the onset of pupation. Cumulative data for the indicated *Or* reporter genes are displayed in the bottom panel, as the average number of *Or*-positive ORNs per antenna or maxillary palp (n = 10–20) in the indicated *dac* loss-of-function background or wild-type. (B) Expression of *Or* genes was examined by semiquantitative RT-PCR on substrate mRNA isolated from antennae or maxillary palps of wild-type (control), *dac<sup>1</sup>/dac<sup>9</sup>* (*dac*), or *en<sup>1</sup>* (*en*) animals. The expression of *Tubulinα<sub>1</sub>* mRNA was included as a control.

(C) Requirement of *en*<sup>+</sup> activity for *Or* gene expression in the anterior compartment. The *ci-GAL4* driver was used to selectively target *UAS-en<sup>hpn</sup>* expression to the anterior compartment in animals bearing the indicated *Or* reporter constructs.

Top panels: Late pupal stage antenna specimens examined on opposite faces for *Or* reporter expression (green color) in the anterior (a) and posterior (p) compartments. *En* gene expression is selectively lost from the anterior compartment in animals bearing *ci-GAL4 > UAS-en<sup>hpn</sup>* (white arrows, bottom row). *Or49b*, expressed only in the posterior compartment, is unaffected. All neurons are stained with anti-Elav (red). *En*-positive ORNs (for *Or49b* wild-type, *wt*) are marked by *en-lacZ* (blue color).

Bottom: Average number of *Or*-positive ORNs in wild-type and *ci-GAL4 > UAS-en<sup>hpn</sup>* animals for *Or* genes expressed in both compartments (ant/pos) or only in the posterior (pos) compartment. To temporally map the requirement for *en*<sup>+</sup>, *ci-GAL4 > UAS-en<sup>hpn</sup>; tubα<sub>1</sub>-GAL80<sup>ts</sup>* animals were shifted to nonpermissive temperature at the onset of pupation (130 hr AEL; red bar) or 12 hr later (12 hr APF; blue bar) to inactivate *GAL80<sup>ts</sup>* and induce *engrailed* RNAi. The number of *Or56a*-positive ORNs was most strongly reduced by early *en* RNAi.

Endo et al. (2007) have observed coincident clonal labeling of ORNs within a single sensillum, consistent with their derivation from a single progenitor. However, other work suggests that sensillum assembly occurs via recruitment initiated by an FC (Ray and Rodrigues, 1995; Reddy et al., 1997). A resolution to these conflicting proposals might be that clonally marked precursors are locally recruited into a nascent sensillum, which migrates into an unmarked field. The labeled sensillum could appear to be the product of a single progenitor, though this is not the case.

Our data do not distinguish between active or passive dispersal mechanisms. Passive dispersal might occur in an environment of strong intrasensillum adhesion, where weak intersensillum adhesion would permit sensillum movement to be powered by tissue-level mechanical forces. However, the large distances over which sensilla move in relation to the epidermis and to other examples of cell movement (Figure 2A) might be more easily explained by an active mechanism. Neuronal migration is well documented in insects (Copenhaver and Taghert, 1989; Ganfornina et al., 1996; Klämbt et al., 1991). In *Drosophila*, stereotyped movement has long been known for glia and neurons (Salzberg et al., 1994; reviewed by Edenfeld et al., 2005). These migrations occur for isolated neurons and small neuronal clusters in patterns regulated by positional cues, such as Wingless, Ephrin, and Slit (Bhat 2007; Coate et al., 2007; Kraut and Zinn, 2004). Recently, complex patterns of mass neuronal movement have been documented in the developing *Drosophila* optic lobe (Hasegawa et al., 2011; Morante et al., 2011). This latter example of neuronal movement, which follows the determination of neuronal identities, most closely resembles the movement of sensilla in the olfactory epithelium. In preliminary work we have found that sensilla follow stereotyped migratory trajectories under the control of secreted molecular signals (E.S., B.d.B., and S.K., unpublished data). Thus, a highly choreographed dispersal mechanism may underlie the development of the *Drosophila* odorant receptor pattern.

The antenna is composed of anterior and posterior compartments whose border was delineated by mosaic analysis (Morata and Lawrence, 1979). We asked whether the motile sensilla respect this border, examining their clonal origin relative to expression of the posterior identity determinant Engrailed (Garcia-Bellido and Santamaria, 1972; Morata and Lawrence, 1975; Kornberg, 1981). Though we found En-positive sensilla in the anterior compartment, and En-negative sensilla in the posterior compartment (Figure 4), mosaic analysis revealed these sensilla to have originated within their resident compartments (Figure 5). Evidently, there was a compartmental switch in expression of Engrailed during sensillum development.

Sensilla arise in a temporal process that begins with the appearance of FCs in concentrically arranged domains orthogonal to the proximal-distal axis of the mature antenna (Figure 3;

Ray and Rodrigues, 1995; Reddy et al., 1997). Engrailed was expressed in the FCs of the inner domain. A subset of these FCs expressed the transcription factor Dachshund (Figure 3). This stereotyped spatial pattern was disrupted as sensilla dispersed across the epithelium (Figures 3H and 4). Though we did not observe this movement in real time, the early and late En-positive sensilla could be connected through the perdurance of a photo-switched fluorescent protein (Figure 5) and the early *en*<sup>+</sup> requirement for *Or* gene expression in En-positive sensilla (Figure 7C).

The pattern of En and Dac expression in mature ORNs was strictly correlated with the expression of specific *Or* genes (Figure 6). Notably, En or Dac expression was not coincident with specific sensillum morphological types or patterns of ORN axonal connectivity (Figure S2). Generally, the ORNs of a sensillum shared their state of En and Dac expression. This overall homogeneity suggests that En and Dac are determinants of sensillum identity, and that downstream processes specify ORN identity and *Or* gene choice (see Endo et al., 2007). If En and Dac participate in a combinatorial code for sensillum identity, three additional regulators would be required to define the 17 characterized sensillum types.

Consistent with such a role, *en* and *dac* loss-of-function resulted in selective loss of *Or* gene expression in En-positive and Dac-positive neurons, respectively (Figure 7; Figure S3). Our analysis could not clearly discern whether this loss of expression was associated with transformation to alternative sensillum identities, though in a few cases, the expression of En-negative or Dac-negative *Or* genes was increased (e.g., *Or59b* and *Or67b*; Figures 7B and S3B). We also asked whether *en*<sup>+</sup> could play an instructive role in sensillum identity. When expressed early, ectopic *en*<sup>+</sup> brought about a partial transformation of the pb1 sensillum identity to pb2. Interestingly, another *Or* regulator, *Pdm3*, yields a similar loss-of-function phenotype (Tichy et al., 2008). Indeed, we found that ectopic *en*<sup>+</sup> strongly reduced *Pdm3* expression (Figure S3F), consistent with the proposal that *en*<sup>+</sup> acts upstream of *Pdm3*.

These observations are consistent with the notion that *Drosophila* *Or* gene expression is regulated by a combinatorial transcription factor code (Ray et al., 2007; Clyne et al., 1999; Tichy et al., 2008; reviewed by Fuss and Ray, 2009). The Pit-1, Oct1/Oct2, and Unc-86 (POU) domain proteins Acj6 and Pdm3 are expressed in a large fraction of ORNs and selectively required for *Or* gene expression. *acj6* is required for nine of the fifteen *Or* genes expressed in Acj6-positive ORNs; *pdm3* is required for one of the four *Or* genes expressed in Pdm3-positive maxillary palp ORNs. By comparison, our data suggest that En and Dac are more uniformly required in En-positive and Dac-positive ORNs. Whereas Acj6 and Pdm3 promoter binding sites are essential for *Or* promoter activity (Tichy et al., 2008; Bai et al., 2009), whether En or Dac might act as directly is unclear. Clustering of consensus Engrailed binding sites

(D) Instructive role of *en*<sup>+</sup> in *Or* choice. Ectopic *en*<sup>+</sup> was expressed with *dac-GAL4 > UAS-en*<sup>+</sup> under temporal control by *tub $\alpha$ 1-GAL80<sup>ts</sup>*. Animals were shifted to 30°C to inactivate *GAL80<sup>ts</sup>* at 6 hr APF.

Top: Confocal micrographs at similar focal planes of maxillary palps, in specimens as described above. *Or* reporter genes are as indicated (anti-GFP; green color). All neurons are labeled by anti-Elav (red color).

Bottom: Average number of *Or*-positive ORNs per maxillary palp. Color code (filled circles, green, red, or yellow) in all panels, indicates pattern of En and Dac expression, as defined in Figure 6. In all panels, error bars represent SEM. For statistical significance; \**p* < 0.05; \*\**p* < 0.01; \*\*\**p* < 0.001.

upstream of  $en^+$ -dependent *Or* genes has not been observed (data not shown). Dac binding sites are as yet undefined. Alternatively, En and/or Dac might act as upstream determinants, as suggested by the role of  $en^+$  as a regulator of *pdm3* (Figure S3F).

It is generally thought that stochastic mechanisms underlie the dispersed patterns of *Or* gene expression. One such mechanism has been described in which the *H* locus, a distal enhancer domain, acts on a restricted set of odorant receptor genes (Lomvardas et al., 2006; Serizawa et al., 2003). However, it is also evident that many *Or* genes are controlled by unique sets of transcriptional regulators acting on complex *cis*-promoter regions. This has raised the question of how an individual sensory neuron selects a regulatory program that is distinct from its neighbors. Our data suggest that, for *Drosophila*, this question might be resolved within the established framework of positional determinants employed in developmental patterning. We suppose that stochastic mechanisms might still act locally in the spatially stereotyped development of nascent sensilla but do not find such mechanisms necessary to explain the dispersed patterns of *Drosophila Or* gene expression.

## EXPERIMENTAL PROCEDURES

### Lineage and Mosaic Analysis

FLP intramolecular recombination-activated *lacZ* and *GAL4* drivers (Pignoni and Zipursky, 1997; Struhl and Basler, 1993) were used to generate *lacZ*- or GFP-labeled clones, respectively, in animals of the genotypes:

$$P\{hsp70\text{-FLP}\}122; P\{tub_{\alpha1} > y^+, CD2 > GAL4\}/P\{w^+, UAS\text{-}CD8::GFP\}$$

$$P\{hsp70\text{-FLP}\}122; P\{Act5C > CD2 > GAL4\}/P\{w^+, UAS\text{-}CD8::GFP\}$$

$$P\{hsp70\text{-FLP}\}122; P\{Act5C > y^+ > lacZ\}$$

The symbol > indicates an FRT recombination site.

MARCM lineage analysis was carried out as described by Lee and Luo (1999). Animals were of the genotypes:

$$w^+, P\{GawB\}elav^{C155}, P\{hsp70\text{-FLP}\}1/y, w^{1118}, P\{hsp70\text{-FLP}\}1; P\{FRT(w[hs])\}42B, P\{tub_{\alpha1}\text{-}GAL80\}/P\{FRT(w[hs])\}42B, P\{w^+, UAS\text{-}CD8::GFP\}$$

$$P\{hsp70\text{-FLP}\}1, y^1, w^{1118}/y, w^*; P\{FRT(w[hs])\}42B, P\{tub_{\alpha1}\text{-}GAL80\}/P\{FRT(w[hs])\}42B, P\{w^+, UAS\text{-}mCD8::GFP\}; P\{tub_{\alpha1}\text{-}GAL4\}/+$$

Animals of the above genotypes were grown to developmental stages indicated and subjected to heat-shocks calibrated to yield infrequent recombination events so that most specimens contained one or no clone (see Supplemental Experimental Procedures). The animals were then returned to normal growth conditions until antennae were removed for analysis at the indicated times.

### Mutant Analysis

Animals carrying *dachshund* alleles,  $dac^1$  and  $dac^9$ , or the *engrailed* alleles,  $en^1$  and  $en^{54}$ , were crossed to individual *Or* gene reporter lines (Table S1) to construct the following strains:

$$dac^9/dac^1; P\{Or\text{-}GFP\}$$

$$dac^9, P\{Or\text{-}GFP\}/dac^1$$

$$en^1/en^1; P\{Or\text{-}GFP\}$$

$$en^1, P\{Or\text{-}GFP\}/en^1$$

$$y, w, P\{w^+, UAS\text{-}CD8::GFP\}; dac^9/dac^1; P\{Or\text{-}GAL4\}$$

$$y, w, P\{w^+, UAS\text{-}CD8::GFP\}; dac^9, P\{Or\text{-}GAL4\}/dac^1$$

$$y, w, P\{w^+, UAS\text{-}CD8::GFP\}; en^1/en^1; P\{Or\text{-}GAL4\}$$

$$en^{54}/en^{54} \text{ (for RT-PCR)}$$

Antennae were removed from late-pupal/adult-stage animals and processed for immunohistochemistry or RT-PCR.

### Transgene Expression

To target RNAi specifically to anterior compartments,  $P\{w^+, UAS\text{-}en^{hpm}\}$  was driven by  $P\{w^+, ci\text{-}GAL4\}$  in the presence of various *Or* gene expression reporters (Table S1):  $P\{w^+, ci\text{-}GAL4\}$ ;  $P\{w^+, UAS\text{-}en^{hpm}\}/P\{Or\text{-}GFP\}$ . Ectopic expression of  $P\{w^+, UAS\text{-}en^+\}$  or  $P\{w^+, UAS\text{-}dac^{hpm}\}$  driven by  $P\{en2.4\text{-}GAL4\}^{e16E}$  or  $P\{GawB\}dac$  was also temporally controlled with  $P\{w^+, tub_{\alpha1}\text{-}GAL80^{ts}\}$  in order to avoid early developmental lethality. Animals were grown at 17°C (permissive temperature for *GAL80<sup>ts</sup>*) until the late third larval instar, when growth temperature was shifted to nonpermissive 30°C:

$$w^*; P\{w^+, tub_{\alpha1}\text{-}GAL80^{ts}\}; P\{GawB\}dac/P\{w^+, UAS\text{-}dac^{hpm}\}, P\{Or\text{-}GFP\}$$

$$w^*; P\{w^+, tub_{\alpha1}\text{-}GAL80^{ts}\}; P\{en2.4\text{-}GAL4\}^{e16E}/P\{w^+, UAS\text{-}en^+\}, P\{Or\text{-}GFP\}$$

### Microscopy and Data Analysis

Image data was acquired on a Zeiss LSM510 Meta confocal microscope and processed with ImageJ. Error estimates in all figure panels are SEM (for \*,  $p < 0.05$ ; for \*\*,  $p < 0.01$ ; for \*\*\*,  $p < 0.001$ ).

### SUPPLEMENTAL INFORMATION

Supplemental Information includes three figures, one table, Supplemental Experimental Procedures, and two movies and can be found with this article online at doi:10.1016/j.devcel.2011.12.015.

### ACKNOWLEDGMENTS

We are indebted to B. Dickson (IMP) and L. Vosshall (Rockefeller) for *Or* transgenic reagents and to Dr. H. Aberle (HHU) for sharing unpublished information. We also thank G. Struhl (Columbia), R. Holmgren (Northwestern), G. Mardon (Baylor), and the Bloomington *Drosophila* Stock Center for strains and reagents.

Received: February 4, 2011

Revised: October 24, 2011

Accepted: December 20, 2011

Published online: February 13, 2012

### REFERENCES

- Ando, R., Hama, H., Yamamoto-Hino, M., Mizuno, H., and Miyawaki, A. (2002). An optical marker based on the UV-induced green-to-red photoconversion of a fluorescent protein. *Proc. Natl. Acad. Sci. USA* 99, 12651–12656.
- Bai, L., Goldman, A.L., and Carlson, J.R. (2009). Positive and negative regulation of odor receptor gene choice in *Drosophila* by *acj6*. *J. Neurosci.* 29, 12940–12947.
- Benton, R., Vannice, K.S., Gomez-Diaz, C., and Vosshall, L.B. (2009). Variant ionotropic glutamate receptors as chemosensory receptors in *Drosophila*. *Cell* 136, 149–162.
- Bhat, K.M. (2007). Wingless activity in the precursor cells specifies neuronal migratory behavior in the *Drosophila* nerve cord. *Dev. Biol.* 311, 613–622.
- Blagburn, J.M. (2008). Engrailed expression in subsets of adult *Drosophila* sensory neurons: an enhancer-trap study. *Invert. Neurosci.* 8, 133–146.
- Chou, Y.H., Zheng, X., Beachy, P.A., and Luo, L. (2010). Patterning axon targeting of olfactory receptor neurons by coupled hedgehog signaling at two distinct steps. *Cell* 142, 954–966.
- Clyne, P., Grant, A., O'Connell, R., and Carlson, J.R. (1997). Odorant response of individual sensilla on the *Drosophila* antenna. *Invert. Neurosci.* 3, 127–135.
- Clyne, P.J., Certel, S.J., de Bruyne, M., Zaslavsky, L., Johnson, W.A., and Carlson, J.R. (1999). The odor specificities of a subset of olfactory receptor neurons are governed by *Acj6*, a POU-domain transcription factor. *Neuron* 22, 339–347.
- Coate, T.M., Swanson, T.L., Proctor, T.M., Nighorn, A.J., and Copenhaver, P.F. (2007). Eph receptor expression defines midline boundaries for ephrin-positive migratory neurons in the enteric nervous system of *Manduca sexta*. *J. Comp. Neurol.* 502, 175–191.

- Copenhaver, P.F., and Taghert, P.H. (1989). Development of the enteric nervous system in the moth. II. Stereotyped cell migration precedes the differentiation of embryonic neurons. *Dev. Biol.* **131**, 85–101.
- Couto, A., Alenius, M., and Dickson, B.J. (2005). Molecular, anatomical, and functional organization of the *Drosophila* olfactory system. *Curr. Biol.* **15**, 1535–1547.
- Davis, R.L. (2005). Olfactory memory formation in *Drosophila*: from molecular to systems neuroscience. *Annu. Rev. Neurosci.* **28**, 275–302.
- de Bruyne, M., Clyne, P.J., and Carlson, J.R. (1999). Odor coding in a model olfactory organ: the *Drosophila* maxillary palp. *J. Neurosci.* **19**, 4520–4532.
- de Bruyne, M., Foster, K., and Carlson, J.R. (2001). Odor coding in the *Drosophila* antenna. *Neuron* **30**, 537–552.
- Dobritsa, A.A., van der Goes van Naters, W., Warr, C.G., Steinbrecht, R.A., and Carlson, J.R. (2003). Integrating the molecular and cellular basis of odor coding in the *Drosophila* antenna. *Neuron* **37**, 827–841.
- Edenfeld, G., Stork, T., and Klämbt, C. (2005). Neuron-glia interaction in the insect nervous system. *Curr. Opin. Neurobiol.* **15**, 34–39.
- Elkins, T., Hortsch, M., Bieber, A.J., Snow, P.M., and Goodman, C.S. (1990). *Drosophila* fasciclin I is a novel homophilic adhesion molecule that along with fasciclin III can mediate cell sorting. *J. Cell Biol.* **110**, 1825–1832.
- Elmore, T., Ignell, R., Carlson, J.R., and Smith, D.P. (2003). Targeted mutation of a *Drosophila* odor receptor defines receptor requirement in a novel class of sensillum. *J. Neurosci.* **23**, 9906–9912.
- Endo, K., Aoki, T., Yoda, Y., Kimura, K., and Hama, C. (2007). Notch signal organizes the *Drosophila* olfactory circuitry by diversifying the sensory neuronal lineages. *Nat. Neurosci.* **10**, 153–160.
- Fishilevich, E., and Vosshall, L.B. (2005). Genetic and functional subdivision of the *Drosophila* antennal lobe. *Curr. Biol.* **15**, 1548–1553.
- Fuss, S.H., and Ray, A. (2009). Mechanisms of odorant receptor gene choice in *Drosophila* and vertebrates. *Mol. Cell. Neurosci.* **41**, 101–112.
- Fuss, S.H., Omura, M., and Mombaerts, P. (2007). Local and cis effects of the H element on expression of odorant receptor genes in mouse. *Cell* **130**, 373–384.
- Ganforina, M.D., Sánchez, D., and Bastiani, M.J. (1996). Embryonic development of the enteric nervous system of the grasshopper *Schistocerca americana*. *J. Comp. Neurol.* **372**, 581–596.
- García-Bellido, A., and Santamaria, P. (1972). Developmental analysis of the wing disc in the mutant *engrailed* of *Drosophila melanogaster*. *Genetics* **72**, 87–104.
- Goldman, A.L., Van der Goes van Naters, W., Lessing, D., Warr, C.G., and Carlson, J.R. (2005). Coexpression of two functional odor receptors in one neuron. *Neuron* **45**, 661–666.
- Hallem, E.A., and Carlson, J.R. (2006). Coding of odors by a receptor repertoire. *Cell* **125**, 143–160.
- Hallem, E.A., Ho, M.G., and Carlson, J.R. (2004). The molecular basis of odor coding in the *Drosophila* antenna. *Cell* **117**, 965–979.
- Hasegawa, E., Kitada, Y., Kaido, M., Takayama, R., Awasaki, T., Tabata, T., and Sato, M. (2011). Concentric zones, cell migration and neuronal circuits in the *Drosophila* visual center. *Development* **138**, 983–993.
- Hoppe, R., Frank, H., Breer, H., and Strotmann, J. (2003). The clustered olfactory receptor gene family 262: genomic organization, promoter elements, and interacting transcription factors. *Genome Res.* **13**, 2674–2685.
- Hoppe, R., Breer, H., and Strotmann, J. (2006). Promoter motifs of olfactory receptor genes expressed in distinct topographic patterns. *Genomics* **87**, 711–723.
- Klämbt, C., Jacobs, J.R., and Goodman, C.S. (1991). The midline of the *Drosophila* central nervous system: a model for the genetic analysis of cell fate, cell migration, and growth cone guidance. *Cell* **64**, 801–815.
- Kornberg, T. (1981). *Engrailed*: a gene controlling compartment and segment formation in *Drosophila*. *Proc. Natl. Acad. Sci. USA* **78**, 1095–1099.
- Kraut, R., and Zinn, K. (2004). Roundabout 2 regulates migration of sensory neurons by signaling in trans. *Curr. Biol.* **14**, 1319–1329.
- Larsson, M.C., Domingos, A.I., Jones, W.D., Chiappe, M.E., Amrein, H., and Vosshall, L.B. (2004). Or83b encodes a broadly expressed odorant receptor essential for *Drosophila* olfaction. *Neuron* **43**, 703–714.
- Lawrence, P.A., and Green, S.M. (1979). Cell lineage in the developing retina of *Drosophila*. *Dev. Biol.* **71**, 142–152.
- Lawrence, P.A., and Struhl, G. (1982). Further studies of the *engrailed* phenotype in *Drosophila*. *EMBO J.* **1**, 827–833.
- Lecuit, T., and Cohen, S.M. (1997). Proximal-distal axis formation in the *Drosophila* leg. *Nature* **388**, 139–145.
- Lee, T., and Luo, L. (1999). Mosaic analysis with a repressible cell marker for studies of gene function in neuronal morphogenesis. *Neuron* **22**, 451–461.
- Lomvardas, S., Barnea, G., Pisapia, D.J., Mendelsohn, M., Kirkland, J., and Axel, R. (2006). Interchromosomal interactions and olfactory receptor choice. *Cell* **126**, 403–413.
- Mardon, G., Solomon, N.M., and Rubin, G.M. (1994). *dachshund* encodes a nuclear protein required for normal eye and leg development in *Drosophila*. *Development* **120**, 3473–3486.
- Morante, J., Erclik, T., and Desplan, C. (2011). Cell migration in *Drosophila* optic lobe neurons is controlled by *eyeless/Pax6*. *Development* **138**, 687–693.
- Morata, G., and Lawrence, P.A. (1975). Control of compartment development by the *engrailed* gene in *Drosophila*. *Nature* **255**, 614–617.
- Morata, G., and Lawrence, P.A. (1978). Anterior and posterior compartments in the head of *Drosophila*. *Nature* **274**, 473–474.
- Morata, G., and Lawrence, P.A. (1979). Development of the eye-antenna imaginal disc of *Drosophila*. *Dev. Biol.* **70**, 355–371.
- Ngai, J., Chess, A., Dowling, M.M., Necles, N., Macagno, E.R., and Axel, R. (1993). Coding of olfactory information: topography of odorant receptor expression in the catfish olfactory epithelium. *Cell* **72**, 667–680.
- Pignoni, F., and Zipursky, S.L. (1997). Induction of *Drosophila* eye development by *decapentaplegic*. *Development* **124**, 271–278.
- Ray, K., and Rodrigues, V. (1995). Cellular events during development of the olfactory sense organs in *Drosophila melanogaster*. *Dev. Biol.* **167**, 426–438.
- Ray, A., van Naters, W.G., Shiraiwa, T., and Carlson, J.R. (2007). Mechanisms of odor receptor gene choice in *Drosophila*. *Neuron* **53**, 353–369.
- Ray, A., van der Goes van Naters, W., and Carlson, J.R. (2008). A regulatory code for neuron-specific odor receptor expression. *PLoS Biol.* **6**, e125.
- Ready, D.F., Hanson, T.E., and Benzer, S. (1976). Development of the *Drosophila* retina, a neurocrystalline lattice. *Dev. Biol.* **53**, 217–240.
- Reddy, G.V., Gupta, B., Ray, K., and Rodrigues, V. (1997). Development of the *Drosophila* olfactory sense organs utilizes cell-cell interactions as well as lineage. *Development* **124**, 703–712.
- Ressler, K.J., Sullivan, S.L., and Buck, L.B. (1993). A zonal organization of odorant receptor gene expression in the olfactory epithelium. *Cell* **73**, 597–609.
- Salzberg, A., D'Evelyn, D., Schulze, K.L., Lee, J.K., Strumpf, D., Tsai, L., and Bellen, H.J. (1994). Mutations affecting the pattern of the PNS in *Drosophila* reveal novel aspects of neuronal development. *Neuron* **13**, 269–287.
- Sato, K., Pellegrino, M., Nakagawa, T., Nakagawa, T., Vosshall, L.B., and Touhara, K. (2008). Insect olfactory receptors are heteromeric ligand-gated ion channels. *Nature* **452**, 1002–1006.
- Serizawa, S., Miyamichi, K., Nakatani, H., Suzuki, M., Saito, M., Yoshihara, Y., and Sakano, H. (2003). Negative feedback regulation ensures the one receptor-one olfactory neuron rule in mouse. *Science* **302**, 2088–2094.
- Shanbhag, S.R., Müller, B., and Steinbrecht, R.A. (2000). Atlas of olfactory organs of *Drosophila melanogaster* 2. Internal organization and cellular architecture of olfactory sensilla. *Arthropod Struct. Dev.* **29**, 211–229.
- Struhl, G., and Basler, K. (1993). Organizing activity of wingless protein in *Drosophila*. *Cell* **72**, 527–540.
- Tichy, A.L., Ray, A., and Carlson, J.R. (2008). A new *Drosophila* POU gene, *pdm3*, acts in odor receptor expression and axon targeting of olfactory neurons. *J. Neurosci.* **28**, 7121–7129.
- Vassar, R., Ngai, J., and Axel, R. (1993). Spatial segregation of odorant receptor expression in the mammalian olfactory epithelium. *Cell* **74**, 309–318.

- Vosshall, L.B., Amrein, H., Morozov, P.S., Rzhetsky, A., and Axel, R. (1999). A spatial map of olfactory receptor expression in the *Drosophila* antenna. *Cell* 96, 725–736.
- Wicher, D., Schäfer, R., Bauernfeind, R., Stensmyr, M.C., Heller, R., Heinemann, S.H., and Hansson, B.S. (2008). *Drosophila* odorant receptors are both ligand-gated and cyclic-nucleotide-activated cation channels. *Nature* 452, 1007–1011.
- Yao, C.A., Ignell, R., and Carlson, J.R. (2005). Chemosensory coding by neurons in the coeloconic sensilla of the *Drosophila* antenna. *J. Neurosci.* 25, 8359–8367.
- Zinn, K., McAllister, L., and Goodman, C.S. (1988). Sequence analysis and neuronal expression of fasciclin I in grasshopper and *Drosophila*. *Cell* 53, 577–587.